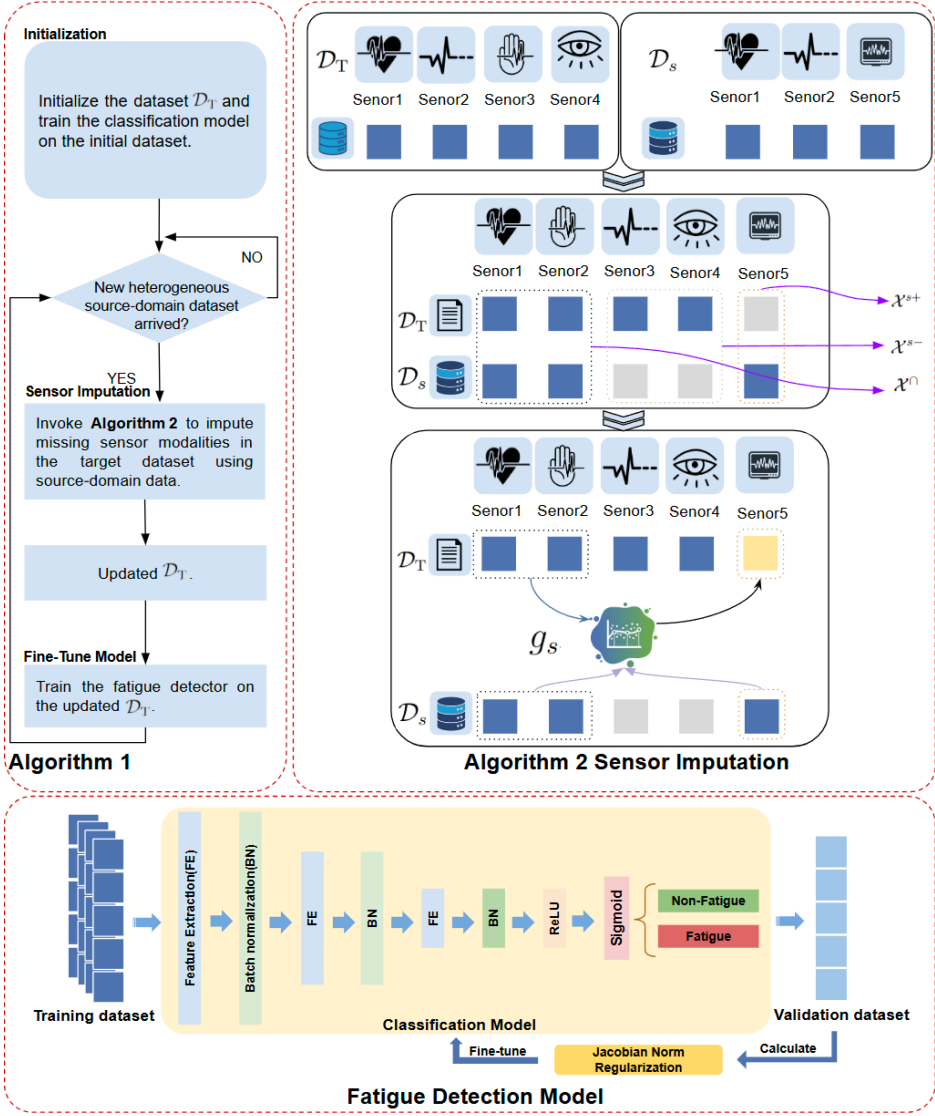


# Graphical Abstract

## Leveraging multi-source and heterogeneous signals for fatigue detection

Luobin Cui, Yanlai Wu, Tang Ying, Weikai Li



## Highlights

### **Leveraging multi-source and heterogeneous signals for fatigue detection**

Luobin Cui, Yanlai Wu, Tang Ying, Weikai Li

- We propose a practical, multi-source fatigue detection framework that addresses the challenge of leveraging high-fidelity knowledge from differently instrumented sensor domains to improve fatigue predication in real-world settings. The framework dynamically aligns heterogeneous signals across overlapping fatigue-related feature spaces, infers missing sensor modalities through targeted imputation, and continuously refines predictions under realistic, constrained sensing conditions.
- Comprehensive experiments based on a realistic, field-deployed sensor configuration—augmented with two publicly available benchmark datasets—demonstrate the framework’s effectiveness in leveraging cross-domain data, its robustness to differences in sensor modality, and significant improvement in fatigue detection accuracy under practical, sensor-limited scenarios

# Leveraging multi-source and heterogeneous signals for fatigue detection

Luobin Cui<sup>a</sup>, Yanlai Wu<sup>a</sup>, Tang Ying<sup>a</sup>, Weikai Li<sup>b</sup>

<sup>a</sup>*Rowan University, 201 Mullica Hill Rd, Glassboro, 08028, NJ, USA*

<sup>b</sup>*College of Mathematics and Statistics, Chongqing Jiaotong University, 66 Xuefu Blvd, Nan'An, Chongqing, 400074, China*

---

## Abstract

Fatigue detection plays a critical role in safety-critical applications such as aviation, mining, and long-haul transport. However, most existing methods rely on high-end sensors and controlled environments, limiting their applicability in real-world settings. This paper formally defines a practical yet underexplored problem setting for real-world fatigue detection, where systems operating with context-appropriate sensors aim to leverage knowledge from differently instrumented sources—including those using impractical sensors deployed in controlled environments. To tackle this challenge, we propose a heterogeneous and multi-source fatigue detection framework that adaptively utilizes the available modalities in the target domain while benefiting from the diverse configurations present in source domains. Our experiments, conducted using a realistic field-deployed sensor setup and two publicly available datasets, demonstrate the practicality, robustness, and improved generalization of our approach, paving the practical way for effective fatigue monitoring in sensor-constrained scenarios.

*Keywords:*

fatigue detection, sensor imputation, data synthesis

---

## 1. Introduction

Physiological responses and behavioral patterns of individuals under fatigue provide rich information to understand the impacts of jeopardized human capacity, from which proper mitigation control can be determined. However, the complexity and vulnerability of data acquisition presents several limitations. While the latest advancements of sensor technology have

elevated the research of objective fatigue detection to unprecedented levels, concerns about sensor reliability and accessibility remain [1].

Unreliable sensors can result in loss of data, compromising detection accuracy, or, in the worst case, complete malfunction. To address this issue, recent efforts have explored using synthetic data generation strategies to augment limited or incomplete datasets. For instance, generative AI [2] has emerged as a promising solution. Bird et al. (2021) demonstrated the capability of GPT-2 in generating synthetic Electroencephalography (EEG) and Electromyography (EMG), which, when combined with real training data, improved classification accuracy [3]. Similarly, research in [4] employed generative adversarial networks (GAN) to enhance data for motor imagery classification in brain-computer interface systems. Along this direct, [5] proposed Generative-DANN (GDANN), a hybrid model that integrates GANs with a Domain-Adversarial Neural Network (DANN) architecture to address cross-subject EEG variability in fatigue detection. By aligning feature distributions across subjects, GDANN improved generalizability and achieved high accuracy in cross-subject fatigue classification tasks. When generating synthetic data for fatigue detection, the process must consider inherent correlations of physiological modalities to collaboratively determine fatigue. To that end, RAINDROP [6] provided a promising approach by using graph neural networks to model these correlations in irregularly sampled and multivariate time-series data.

Although the aforementioned approaches address the challenge of sensor unreliability through data augmentation, few efforts have tackled the equally critical issue of sensor accessibility. In many real-world scenarios, high-end sensors, while reliable and accurate, remain prohibitively expensive or impractical for broad deployment. As a result, studies involving these sensors are often confined to simulated and controlled environments. For example, high-resolution EEG was deployed in a simulated environment, together with heart rate and eye blinks rate, to analyze mental fatigue or drowsiness during car driving [7]. However, such simulation-based setups often fail to capture the complexity and uncertainty of actual driving conditions [8]. Moreover, these sensors—such as EEG, imaging systems, and pupil dilation monitors—are highly sensitive to environmental factors, including noise, lighting, and field-of-view constraints. These sensitivities complicate data collection and analysis in real-world scenarios, ultimately degrading model accuracy and robustness [9]. This gap presents a compelling opportunity: Can we transfer the high-fidelity knowledge extracted from controlled envi-

ronments—where certain sensors are deployed but unsuitable for real-world use—to practical settings that rely on a different set of context-appropriate sensors? Instead of attempting to replicate the sensor configurations used in laboratory settings, we hypothesize that a novel domain-adaptive framework can be developed to align heterogeneous signal representations, enabling real-world fatigue detection systems to learn from and be enhanced by control-environment data, even if they originate from entirely different sources. Guided by this bold idea, this paper presents a practical fatigue detection solution, and makes the following contributions:

- A practical yet underexplored problem setting for real-world fatigue detection is formally defined. This definition reflects the need to operate fatigue detection systems with context-appropriate sensors in the field and presents the opportunity to augment these systems with knowledge transferred from differently instrumented sensor sources. It ultimately lays the foundation for developing models that are robust to modality heterogeneity, incompleteness, and domain shift.
- A heterogeneous and multi-source fatigue detection framework is proposed as a solution to this problem, supported by a thorough theoretical analysis. In particular, we explore the conditions under which knowledge from differently instrumented source domains can be effectively leveraged to support fatigue prediction in a target domain with incomplete and mismatched sensor modalities. Building on these insights, we then develop a model that adaptively leverages the available modalities in the target domain while benefiting from the diverse modality configurations present across multiple source domains. The design enables accurate fatigue prediction in practical settings, even under constrained sensor configurations, resulting in improved generalization and overall performance.
- The proposed framework is validated through a practical sensor setup together with two publicly available datasets, demonstrating the practicality and robustness of the proposed solution.

## 2. Related Work

This section reviews key developments in fatigue assessment. Section 2.1 examines traditional and modern fatigue detection methods, highlighting their advantages and limitations, which underscore the need for a new

approach that builds on strengths while addressing shortcomings. Section 2.2 explores the current data generation methods in mitigating data scarcity, along with their constraints in practical applications. Finally, Section 2.3 discusses the use of open datasets for fatigue assessment and the challenges associated with their heterogeneity and generalizability.

### *2.1. Traditional and Diversified Fatigue Assessment*

Traditional fatigue assessment methods are based on subjective evaluation tools, including self-reports and questionnaires. Since the last century, numerous classic fatigue assessment scales have been widely utilized, including the Stanford Sleepiness Scale (SSS) [10], proposed by Stanford University; the Multidimensional Fatigue Inventory (MFI) [11], developed by Smets et al.; and the International Fitness Scale (IFIS) [12], which measures changes in overall vigor and affect. These scales encompass a multitude dimensions of fatigue and serves as the foundation for traditional fatigue assessment. Nevertheless, both questionnaires and self-reports are highly influenced by an individual’s psychological state and external environment, resulting in subjective and inconsistent outcomes [13]. Moreover, most of these methods [14, 15, 16] are post-hoc assessments, making them unsuitable for real-time fatigue monitoring and preventive measures-both of which are essential in high-stakes environments, such as driving [17] and aviation [18].

To address these limitations, researchers have explored more objective measures of human fatigue. In fact, a person’s fatigue state can be reflected in changes in physiological signals, such as heart rate (HR), heart rate variability (HRV), electrocardiogram (ECG), electroencephalogram (EEG), galvanic skin response (GSR), skin yemperature (ST), blood pressure(BP), electromyography(EMG) and blood oxygen saturation (SpO2). Studies have shown that when drivers enter a fatigued state, their HRV metrics change significantly. Notably, a decrease is often observed in the time domain on measures such as how much the time between heartbeats naturally varies and how much consecutive heartbeats differ from each other. This suggests that the ability of the body to regulate heart activity is weakened. Similarly, HRV indicators in the frequency domain, such as the low-frequency and high-frequency ratios, often become unstable, reflecting an imbalance in the regulatory function of the autonomic nervous system [19]. Additionally, GSR signals during fatigue are usually characterized by a rise in baseline conductance level and response fluctuations, which is closely correlated

to enhanced sympathetic nerve activities [20]. Through real-time monitoring and joint analysis of these specific indicators, the subtle changes in the driver’s physiological state can be captured more precisely, thus significantly improving the sensitivity and accuracy of the fatigue detection system [21]. With technological advancement, physiological signal acquisition devices are becoming smaller and more user-friendly, significantly driving research in real-time fatigue monitoring [22, 23, 24].

Among various physiological signals, EEG has gained popularity in fatigue detection due to its ability to directly measure brain activity with high accuracy. However, traditional EEG systems are expensive, require an intrusive setup and specialized personnel for operation, making it challenging for real-world deployment. As a result, the majority of EEG-based fatigue studies remain confined to controlled laboratory settings [25, 26, 27]. Although portable EEG devices have emerged for field applications, their data quality is not as good as that of laboratory-grade devices. Additionally, they are susceptible to external noise and interference, significantly impacting their stability and detection accuracy [28, 29].

In response to these challenging, researchers have explored non-invasive alternatives, leading to the rise of vision-based fatigue detection.

These methods assess fatigue by analyzing facial features [30], such as eyelid closure time [31], yawning frequency [32], facial feature [33], and head movement [34] from images captured by cameras in real time. Despite their many advantages, these methods also face challenges, such as lighting variations and camera angles, which can affect image quality, and ultimately detection accuracy. In addition, long-term monitoring human subjects’ facial and body movements in work environments raises privacy concerns [35] and may lead to employee resistance. Along with this trend, alternative visual signals, like pupil dilation and gaze tracking, have gained attention in the field of fatigue detection. Eyes are often considered as the most intuitive window of mental state, which can directly reflect the immediate response to fatigue and show high accuracy in fatigue assessment. Studies have shown that pupil diameter and gaze focus are important indicators for assessing workload and fatigue status [36, 37, 38], including our own study [39] to collect human eye and physiological data for combined fatigue detection. However, while pupil dilation and gaze tracking offer promising insights, they are also sensitive to external environmental factors. Pupil dilation can be influenced by ambient lighting conditions, which may reduce its reliability in dynamic or uncontrolled environments. Similarly, gaze tracking can be

affected by head movements, occlusions, and variations in camera positioning, limiting its stability and accuracy unless the camera is confined to a controlled environment, such as the one in our study [39] using Hololens.

In summary, different sensor signals possess distinct advantages in fatigue detection, with some proving more effective than others. However, their effectiveness is highly contingent on applications and settings. For example, EEG is highly effective in controlled environments but impractical for real-world scenarios due to its sensitivity and complex setup requirements. Similar sensitivity issues rule out the use of pupil dilation in practical applications, and require the use of gaze tracking within a confined setup. Therefore, researchers usually select available and/or context-appropriate resources to collect signals that best align with their research objectives. Even so, we should not overlook the value of the knowledge learned from settings where these context-inappropriate sensors have been effectively applied. If a mechanism exists to transfer that knowledge, it could be used to augment fatigue detection in environments where those sensors are unavailable or impractical, thereby preserving their contribution without requiring their direct deployment.

## *2.2. Data Synthesis Methods*

Data synthesis, a technology that generates artificial data that maintains the statistical or structural characteristics of real datasets, has demonstrated significant advantages in dealing with data scarcity in recent years. This is particularly relevant in physiological signal analysis, where data collection can be challenging due to various factors such as sensor availability, sensitivity to noise, and subject-related variability, leading to widespread adoption in this domain.

Early developments in DS primarily leveraged statistical regression techniques, where synthetic data was generated through parameterized modeling of observed data distributions. For instance, Linear regression and Bayesian regression were among the first approaches adopted to model temporal dependencies and fill in missing physiological signals by assuming probabilistic relationships among features [40]. As datasets grew in complexity and dimensionality, regularized models such as ridge regression [41] and lasso regression [42] were introduced to improve generalization. However, despite these advancements, statistical models remained fundamentally limited in their ability to capture long-term dependencies and nonlinear temporal dynamics, which are prevalent in complex physiological signals.

Deep learning, on the other hand, has provided promising solutions to this challenge. Recurrent Neural Networks (RNNs), particularly Long Short-Term Memory (LSTM) networks, have proven effective in capturing long-term temporal dependencies in multivariate time-series data. Several studies have demonstrated their success in a variety of applications, such as GRU-D, which incorporates decay mechanisms and masking for clinical time-series data [43]; an LSTM-based imputation model for ECG signals that outperforms classical methods [44]; and BRITS, which enables bidirectional gradient-based imputation without strong distributional assumptions [45]. In parallel, Convolutional Neural Networks (CNN) have shown great success in extracting local spatial and temporal features. Their strength has inspired hybrid models that combine CNNs with LSTMs to jointly leverage spatial and temporal dependencies for more accurate imputation and signal reconstruction [46]. Additionally, Generative Adversarial Networks (GANs) have emerged as a leading approach for producing high-fidelity synthetic signals that are statistically indistinguishable from real ones. Examples can be found in [47, 48].

Despite this progress, current DS techniques across both classical and deep learning paradigms typically operate under a critical limitation: they rely solely on observed data from a single modality or domain to infer or generate new data of the same type. This assumption restricts their generalizability and limits their ability to model cross-domain relationships or synthesize data from unseen modalities or sources, which is especially problematic in real-world physiological settings, where data is not only sparse and incomplete, but also highly heterogeneous across domains, such as different sensing devices, sensing modalities, and subject populations. Overcoming this constrain is essence of our work, which aims to enable more flexible and adaptive synthesis by integrating knowledge across both domains and modalities.

### *2.3. Open Fatigue Detection Datasets*

A review of relevant literature has identified several open datasets for fatigue detection. As shown in Table 1, the use of diverse physiological signals reaffirms our observation that researchers tend to select those sensors that are readily accessible and convenient for their studies. Meanwhile, we also note that certain signals are commonly used across diverse datasets, including HR, PPG, EDA, Acceleration(ACC) and ST.

The commonality and diversity across datasets present both challenges and opportunities for fatigue detection. For example, while FatigueSet [49], MEFAR [50], and VPFD [39] share similar types of data, they use different sensors as detailed in a later session - Empatica E4 for the first two datasets and Google Pixel Watch 2 for the third. These variations in data collection methods, sensor specifications, and pre-processing techniques can hinder standardization and generalization. FatigueSet [49] and MEFAR [50], collected under controlled laboratory conditions, include high-fidelity signals—such as EEG in both datasets and ECG in FatigueSet—that are often impractical for real-world deployment. In contrast, the VPFD [39] dataset was designed for real-world use and thus relies on more accessible sensors except for EEG and ECG. This distinction directly motivates our evaluation of the central hypothesis posed in the Introduction: Can fatigue-relevant knowledge learned from high-resolution EEG and ECG sources be effectively transferred to enhance fatigue prediction in settings like VPFD, where only context-appropriate sensors are available? In the following sections, we present the results of this exploration.

Table 1: Summary of fatigue detection datasets and acquisition devices

Dataset	Human Subjects	Hours	Data Types										
			PPG	GSR	HR	ST	ACC	EYE	EEG	ECG	EMG	BP	FACE
CogBeacon [51]	19	35						✓					✓
CLAS [52]	62	31	✓	✓	✓					✓			
MePhy [53]	60	8		✓				✓		✓	✓		✓
OperEYEV [54]	10	10			✓			✓				✓	✓
WESAD [55]	15	13	✓	✓	✓	✓	✓			✓	✓		
FatigueSet [49]	12	13	✓	✓	✓	✓	✓		✓	✓			
MEFAR [50]	23	28	✓	✓	✓	✓	✓		✓				
VPFD [39]	4	9	✓	✓	✓	✓	✓	✓					

### 3. Heterogeneous and Multi-source Fatigue Detection Framework

#### 3.1. Problem Definition

We consider a fatigue detection task in the presence of heterogeneous, incomplete, and multi-source sensor data. Specifically, assume there exists:

- A target domain dataset  $\mathcal{D}_T = \{(x_T^{(i)}, y_T^{(i)})\}_{i=1}^{n_T}$  with limited samples, where  $x_T^{(i)} \in \mathbb{R}^{d_T}$  represents the sensor feature vector defined over  $\mathcal{X}_T$

and  $y_T^{(i)} \in \mathcal{Y}$  is the label.  $n_T$  is the number of target samples and  $d_T$  is the number of feature dimensions, i.e., number of sensors.

- A collection of source domains  $\{\mathcal{D}_s\}_{s=1}^S$ , where each  $\mathcal{D}_s = \{(x_s^{(i)}, y_s^{(i)})\}_{i=1}^{n_s}$  contains samples from a different sensor configuration or environment. Each  $x_s^{(i)} \in \mathbb{R}^{d_s}$  defined over  $\mathcal{X}_s$  and  $y_s^{(i)} \in \mathcal{Y}$ .  $S$  is the number of source domains,  $n_s$  is the number of target source samples and  $d_s$  is the number of feature dimensions of  $\mathcal{D}_s$ .

In the context of our problem, **heterogeneous** refers to the differences in the feature spaces and data distributions across different domains. Specifically, the feature spaces (i.e., the set of sensors or features) and the data distributions (i.e., the statistical properties of the data) in the target domain and source domains are not identical. This can be formally defined as follows:

- **Feature Space Heterogeneity:** The feature spaces across different domains are partially but not completely overlapping, meaning that the set of available features (sensors) in the target domain  $\mathcal{D}_T$  and source domains  $\{\mathcal{D}_s\}_{s=1}^S$  share some common modalities, but also contain domain-specific ones. Formally,  $\mathcal{X}_T \neq \mathcal{X}_s$  and  $\mathcal{X}_T \cap \mathcal{X}_s \neq \emptyset$  for  $s = 1, \dots, S$ . Note that scenarios where the feature spaces are entirely disjoint are not considered in this study.
- **Data Distribution Heterogeneity:** The data distributions across different domains are not identical, meaning that the statistical properties of the data in the target domain  $\mathcal{D}_T$  and source domains  $\{\mathcal{D}_s\}_{s=1}^S$  are different. Formally,  $P_T \neq P_s$  for  $s = 1, \dots, S$ , where  $P_T$  and  $P_s$  represent the data distributions of the target and source domains, respectively.

Since the obtained sensors tend to be heterogeneous across different domains in the data collection process. Thus, we have

- $\mathcal{X}^\cap := \mathcal{X}_T \cap \mathcal{X}_s$  (common sensors between  $\mathcal{D}_T$  and  $\mathcal{D}_s$ )
- $\mathcal{X}^{s-} := \mathcal{X}_s \setminus \mathcal{X}_T^\cap$  (sensors present in  $\mathcal{D}_T$  but missing in  $\mathcal{D}_s$ )
- $\mathcal{X}^{s+} := \mathcal{X}_T \setminus \mathcal{X}_s^\cap$  (sensors present in dataset  $\mathcal{D}_s$  but missing in  $\mathcal{D}_T$ )

Here, we assume that each sensor, regardless of its type or modality, is available in at least one domain. Besides, we also have  $\mathbb{P}_T^\cap \neq \mathbb{P}_s^\cap$ , where  $\mathbb{P}_T^\cap$  and  $\mathbb{P}_s^\cap$  is the distribution over  $\mathcal{X}^\cap$  of  $\mathcal{D}_T$  and  $\mathcal{D}_s$ , respectively. Here, our task is to enhance the performance of a fatigue detector  $f$  in the target domain by leveraging data from multiple heterogeneous source domains. Specifically, we aim to improve the fatigue detection accuracy in the target domain by effectively integrating and aligning data from various source domains, despite their heterogeneous feature spaces and data distributions.

### 3.2. Theoretical Analysis

To gain a deeper understanding of the problem and our proposed solution, we theoretically analyze the generalization bound associated with it. For simplicity and ease of understanding, in our theoretical analysis, we only considered one source domain, which can readily extends to multiple source domains without additional conceptual difficulty. For a random variable  $x$  generated from a distribution  $\mathbb{P}$ , we use  $\mathbb{E}_{x \sim \mathbb{P}}$  to denote the expectation taken over  $x$  with distribution  $\mathbb{P}$ . The expected generalization error of the Fatigue Detector  $f(x)$  is  $\mathcal{E}_{\mathbb{P}}(f)$ , while the empirical generalization error is the  $\mathcal{E}_{\hat{\mathbb{P}}}(f)$ .

**Lemma 1.** [56] *Suppose the loss function  $\mathcal{L}(f(x), y)$  is  $R$ -sub-Gaussian under  $x \sim \mathbb{P}$  for all  $y \in \mathcal{Y}$ , then, we have:*

$$\mathcal{E}_{\mathbb{P}}(f) \leq \mathcal{E}_{\hat{\mathbb{P}}}(f) + \sqrt{\frac{2R^2}{n} I(x, y)} \quad (1)$$

where  $n$  is the number of the training samples and  $I(x, y)$  is the mutual information between  $x$  and  $y$ .

**Theorem 1.** *Assume that  $x, a$  are independent of each other,  $x \sim \mathbb{P}, a \sim \mathbb{Q}_a$ , while both being conditionally dependent on variable of  $y$ , Let the composite observation be defined as  $x^+ = [x, a], x^+ \sim \mathbb{P}_+$ , with the incorporating the variable  $a$ , the  $\mathcal{E}_{\mathbb{P}_+}$  have a tighten upper bound than  $\mathcal{E}_{\mathbb{P}}$ , the gap  $G$  is:*

$$G = \Delta + \sqrt{\frac{2R^2}{n}} \left( \sqrt{I(x^+, y)} - \sqrt{I(x, y)} \right) < 0 \quad (2)$$

where  $\Delta = \mathcal{E}_{\hat{\mathbb{P}}_+} - \mathcal{E}_{\hat{\mathbb{P}}}$ . The proof is given in the Appendix. Following **Theorem 1**, it is evident that incorporating label-related features/sensors (i.e.,  $a$ ) can effectively reduce the generalization error bound, thereby enhancing

the generalization performance. **This result validates the critical necessity of incorporating/generating advanced sensors into our fatigue detection task.**

**Theorem 2.** *Given a random variable  $\hat{a}$  generated from a distribution  $\mathbb{Q}_{\hat{a}}$ , and  $\hat{x}^+ = [x, \hat{a}] \sim \mathbb{Q}$ , then we have:*

$$\mathcal{E}_{\mathbb{P}^+}(f) \leq \mathcal{E}_{\hat{\mathbb{Q}}}(f) + \epsilon_{ideal} + d_{\mathcal{H}\Delta\mathcal{H}}(\mathbb{Q}_a, \mathbb{Q}_{\hat{a}}) + \sqrt{\frac{2R^2}{n}I(x, y)} \quad (3)$$

where  $\mathcal{E}_{\hat{\mathbb{Q}}}(f)$  is the empirical generalization error over distribution  $\mathbb{Q}$ ,  $d_{\mathcal{H}\Delta\mathcal{H}}(\mathbb{Q}_a, \mathbb{Q}_{\hat{a}})$  is the  $\mathcal{H}\Delta\mathcal{H}$  distance between  $\mathbb{Q}_a$  and  $\mathbb{Q}_{\hat{a}}$ . The proof is given in the Appendix.

Through **Theorem 1** and **Theorem 2**, it is evident that without additional sensors  $a$ , if the distribution distance between  $\mathbb{Q}_a$  and  $\mathbb{Q}_{\hat{a}}$ , is less than a constant, i.e.,  $d_{\mathcal{H}\Delta\mathcal{H}}(\mathbb{Q}_a, \mathbb{Q}_{\hat{a}}) \leq \left| \sqrt{\frac{2R^2}{n}} \left( \sqrt{I(a, y)} - \sqrt{I(x, y)} \right) - \Delta - \epsilon_{ideal} \right|$ , we can obtain a tighter generalization error bound, thereby improving the generalization performance of the model. **This result validates that generating advanced sensors can enhance the performance of fatigue detection.**

Thus, to effectively enhance model performance, we are motivated to minimize the distributional discrepancy  $d_{\mathcal{H}\Delta\mathcal{H}}(\mathbb{Q}_a, \mathbb{Q}_{\hat{a}})$  between generated sensor  $\hat{a}$  and potential real sensor  $a$  by training a regression model  $g_s : \mathcal{X}^\cap \rightarrow \mathcal{X}^{s+}$  over  $\mathcal{D}_s$ . Since the  $\mathcal{H}\Delta\mathcal{H}$  distance is symmetric, obeys the triangle inequality, and is bounded, we can regard it as a loss function  $\ell$ . Following the current theoretical work, [57]. We easily have the following results.

**Theorem 3.** *Let  $\mathcal{H}$  be a hypothesis class.  $R_s^\ell(g)$  and  $R_T^\ell(g)$  denote the expected loss of loss function  $\ell$  for the source and target domains. for  $g_s^* = \arg \min_{g \in \mathcal{H}} R_s^\ell(g)$  and  $g_T^* = \arg \min_{h \in \mathcal{H}} R_T^\ell(h)$  denoting the ideal hypotheses for the source and target domains, we have*

$$R_T^\ell(g_s) \leq R_S^\ell(g_s, g_s^*) + d_{\mathcal{H}\Delta\mathcal{H}}(\mathbb{P}_T^\cap, \mathbb{P}_s^\cap) + \epsilon, \quad (4)$$

where  $R_S^\ell(g_s, g_s^*) = \mathbb{E}_{x \sim \mathbb{P}_s} \ell(g_s(x), g_s^*(x))$  and  $\epsilon = R_T^\ell(g_T^*) + R_S^\ell(g_T^*, g_s^*)$ . Since  $\hat{a}$  is generated by  $g_s$ . The  $d_{\mathcal{H}\Delta\mathcal{H}}(\mathbb{Q}_a, \mathbb{Q}_{\hat{a}})$  is bounded by  $R_S^\ell(g_s, g_s^*)$  and  $d_{\mathcal{H}\Delta\mathcal{H}}(\mathbb{P}_T^\cap, \mathbb{P}_s^\cap)$ . Following this idea, **to reduce the distributional discrepancy  $d_{\mathcal{H}\Delta\mathcal{H}}(\mathbb{Q}_a, \mathbb{Q}_{\hat{a}})$ , we also require to reduce the distribution gap  $d_{\mathcal{H}\Delta\mathcal{H}}(\mathbb{P}_T^\cap, \mathbb{P}_s^\cap)$ .**

### 3.3. Learning Objective

Motivated by **Theorem 1** and 2, we provide our heterogeneous and multi-source framework. Specifically, given a target domain  $\mathcal{D}_T$ , our learning objective is to detect fatigue with knowledge transferring from multiple source domains (e.g., high-fidelity knowledge extracted from controlled environments)  $\{\mathcal{D}_s\}$  for  $s = 1, \dots, S$ . Here, as a naive attempt, we aim to transfer knowledge by utilizing the remaining domains to generate the missing sensors (i.e.,  $\mathcal{X}^{s+}$ ) in  $\mathcal{D}_s$ . The learning objective is defined as follows:

$$\mathcal{L} = \min_{g_s, f} \underbrace{\sum_{s=1}^S \mathbb{E}_{\mathcal{D}_s} [\mathcal{L}_{rec}(g_s(\mathcal{X}^\cap, \mathcal{X}^{s+}))]}_{\text{Sensor Reconstruction}} + \underbrace{\lambda \mathbb{E}_{\mathcal{D}_T} [\mathcal{L}_{task}(f(\tilde{\mathcal{X}}_T), y)]}_{\text{Task-Aware Detection}} \quad (5)$$

where  $g_s$  is the feature generator for generating  $\mathcal{X}^{s+}$ ,  $f$  is the classifier function for fatigue detection.  $\mathcal{L}_{rec}$  represents the reconstruction loss (e.g., MSE for regression).  $\mathcal{L}_{task}$  denotes the task-specific loss (e.g., MSE for regression, CE for classification),  $\lambda$  is the adaptive coefficients from uncertainty weighting.  $\tilde{\mathcal{X}}_T$  represents the reconstructed data from domain  $\mathcal{D}_T$ . This data has been enhanced or completed using the information generated by the feature generator  $g_s$  from other domains.

Moreover, motivated by **Theorem 3**, a batch normalization step [58], referred as **BatchNorm**, is applied before fusion, to reduce  $d_{\mathcal{H}\Delta\mathcal{H}}(\mathbb{P}_T^\cap, \mathbb{P}_s^\cap)$ . Additionally, to optimize the objective function in Equation 5, particularly the task-specific loss, we adopt the Jacobian Norm Regularization method [59]—referred to as **JacobianNorm** later.

### 3.4. Framework

The overall framework is summarized in Figure 1, with the detailed procedures outlined in Algorithms 1 and 2. Specifically, we propose a proof-of-concept approach that enables cross-domain knowledge integration for improved fatigue detection in heterogeneous sensor settings. Specifically, the method is designed to handle data collected from different sensor configurations with partially overlapping feature spaces. When new data from a different sensor setup becomes available, the framework compares its feature space to that of the target domain. If discrepancies are found—i.e., missing modalities—the method initiates a targeted imputation process to infer the missing signals. The aligned and augmented data is then incorporated into the model to enhance prediction accuracy in the target domain.

---

**Algorithm 1** Multi-source Fatigue Detection

---

**Require:** Target dataset  $\mathcal{D}_T$ , source datasets  $\{\mathcal{D}_s\}_{s=1}^S$

**Ensure:** Detector  $f$  trained on enhanced target data

- 1: **for**  $s = 1$  **to**  $S$  **do**
  - 2:   Compute shared and unshared features:  $\mathcal{X}^{s-}, \mathcal{X}^{s+}$  w.r.t.  $(\mathcal{D}_T, \mathcal{D}_s)$
  - 3:    $\mathcal{D}_T \leftarrow \text{SENSORIMPUTE}(\mathcal{D}_T, \mathcal{D}_s)$
  - 4: **end for**
  - 5: Train detector  $f_\phi$  on final enhanced  $\mathcal{D}_T$
- 

---

**Algorithm 2** SENSORIMPUTE( $\mathcal{D}_T, \mathcal{D}_s$ )

---

**Require:** Reference dataset  $\mathcal{D}_T$ , auxiliary source dataset  $\mathcal{D}_s$

**Ensure:** Updated target dataset  $\mathcal{D}_T$

- 1: Compute modality-difference sets
$$\mathcal{X}^{s-} = \mathcal{X}_T \setminus \mathcal{X}_s, \quad \mathcal{X}^{s+} = \mathcal{X}_s \setminus \mathcal{X}_T$$
  - 2: **if**  $\mathcal{X}^{s+} \neq \emptyset$  **then**
  - 3:   Apply  $g_s$  to impute missing features  $\mathcal{X}^{s+}$  in  $\mathcal{D}_T$  based on  $\mathcal{D}_s$
  - 4: **end if**
  - 5: **return**  $\mathcal{D}_T$
- 

## 4. Experiments

A series of experiments are designed to validate the proposed target-enhancement framework. Section 4.1 details the experimental setup, including the selected dataset, environment, and data preprocessing, while Section 4.2 describes the experimental design and discusses the results.

### 4.1. Experimental Setup

For the experiments to be elaborated on in a later subsection, three datasets containing various physiological signals-some overlapping and others unique-are selected. Meanwhile, three widely used classification methods are chosen, utilizing both individual datasets and the enhanced target data for training. The details of the selected datasets are in Subection 4.1.1. To minimize discrepancies and enhance the usability of these datasets, we perform data preprocessing as described in Subsection 4.1.2, following the introduction of the experimental environment.

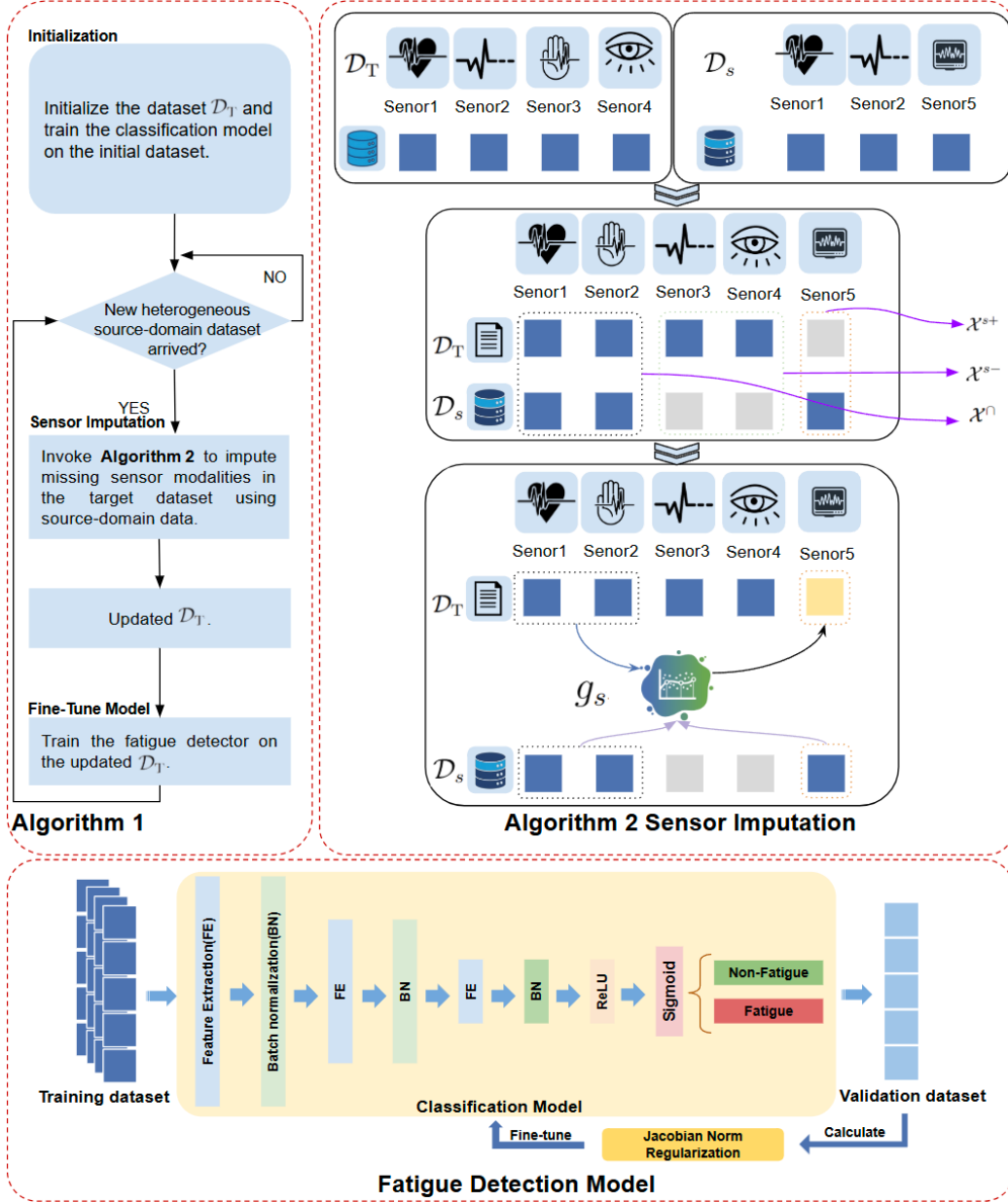


Figure 1: Overall framework

#### 4.1.1. Datasets

Out of all publicly available datasets for fatigue, VPFD[39], MEFAR[50] and FatigueSet[60] are chosen for our experiments because they share a large set of overlapping physiological signals while each also contains unique ones. For instance, all of three datasets include HR, PPG, GSR, ST, and ACC. Additionally, MEFAR provides EEG data, FatigueSet includes both EEG and ECG data, and VPFD offers unique eye-tracking data.

- VPFD dataset[39] is a multimodal fatigue detection dataset designed to reflect practical deployment conditions. It was collected using wearable devices like the HoloLens and Google pixel watch 2. The dataset contains physiological signals from four 27-year-old participants monitored for up to 9 hours during sports, driving, and research activities.
- MEFAR dataset[50] focuses on occupational mental fatigue analysis. It comprises neurophysiological data from 23 participants across four occupational groups (i.e., academicians, technicians, engineers, and kitchen workers). The EEG signals were captured by the NeuroSky MindWave, while other signals were recorded by the Empatica E4 wristband.
- FatigueSet dataset[60] contains data from 12 participants performing controlled physical and cognitive tasks. It utilizes the Muse S headband for EEG signals, the Zephyr BioHarness chestband for ECG signals, and the Empatica E4 wristband for the rest of physiological signals.

#### 4.1.2. Implementation Environment and Data Preprocessing

Experiments are executed on a high-performance PC featuring an Intel Core i9-14900K processor, NVIDIA RTX 4090 GPU, and 128GB of RAM. The system operates on Windows 11, with a software stack comprising Python 3.10.15, PyTorch 2.4.1, scikit-learn 1.1.3, pandas 2.2.2, and numpy 1.26.4.

To minimize noise and artifacts, we apply a series of tailored preprocessing techniques to each signal type. Specifically, ACC and PPG signals are processed using Recursive Least Squares (RLS) and Single-channel Signal Analysis (SSA) to effectively remove motion artifacts while preserving critical physiological features. HR, GSR, and ST signals undergo Maximum Outlier Filtering to eliminate extreme values and ensure data smoothness. Additionally, all signals are resampled to 32 Hz to standardize sampling rates across various devices.

For the FatigueSet dataset, a participant-specific normalization strategy is implemented. Each subject’s data is normalized individually to mitigate inter-subject physiological variability, ensuring that all target-domain samples reside in a unified feature space, thereby enhancing model comparability and training stability.

Before conducting the experiments, we preprocess the dataset and divide it into an 80% training set and a 20% test set using a block-based strategy rather than random splitting. The data is first segmented into continuous blocks based on changes in fatigue labels. For instance, if biometric data is collected from 15 participants, each participant’s data forms a block. From each block, we select 20% of the data for the test set by taking the first 10% and the last 10%. Combined, these selections constitute 20% of the entire dataset, preserving the temporal order and capturing all states without shuffling.

This approach preserves the temporal integrity of the time-series data while maintaining a balanced distribution of fatigue labels, thus ensuring that the test data remained independent of the training process. By preventing test data from being seen during training, this strategy allows for a fair and reliable assessment of model performance while also providing a robust foundation for subsequent model training.

## 4.2. Experimental Design and Results

### 4.2.1. Regression-Based Imputation Model Selection

Without loss of generality, the first set of experiments validates our imputer selection by assessing its ability to recover a single blocked modality. We compare three regression architectures—MLP, LSTM (Long Short-Term Memory), and CNN1D—on two datasets: FatigueSet (with ECG masked) and MEFAR (with EEG masked). In each case, the missing channel is replaced by the model prediction, and we record the mean squared error. Table 2 presents these results. The MLP consistently achieves the lowest loss, demonstrating its superiority as an imputer. Consequently, we employ the MLP for all subsequent modality imputation tasks.

### 4.2.2. Validity of Regression-Imputed Data Versus Noise Baselines

The second set of experiments is designed to not only verify Theorems 1 and 2 but also demonstrate that imputed data can effectively support classifier tasks. In this case, VPFD is chosen with its gaze modality masked and reconstructed using three different methods: MLP-predicted values, MLP

Table 2: Regression performance of different models

	FatigueSet-ECG	MEFAR-EEG
CNN1D	0.5063	0.1031
MLP	0.4074	0.1028
LSTM	0.4250	0.1076

prediction with Gaussian noise, and pure random noise. We refer to the modified datasets as  $\text{VPFD}_{\text{MLP}}$ ,  $\text{VPFD}_{\text{MLP}+\text{noise}}$ , and  $\text{VPFD}_{\text{noise}}$ , respectively. The added noise follows a zero-mean Gaussian distribution whose standard deviation is twice the largest absolute value in the original VPFD gaze data. Finally, we train four separate MLP classifiers using 80% of the original VPFD dataset and each of the three modified versions, respectively. All models are evaluated on the same test set—20% of the original VPFD data—to ensure a consistent basis for comparison. Table 3 clearly shows that the classifier trained on regression-generated data maintains a similar performance to the one trained on the original data. This demonstrates the potential of data synthesis as a solution for addressing missing data. However, the introduction of noise, whether partial or complete, increases the distribution difference between the original and generated data, leading to degraded classifier performance.

Table 3: Classification performance on different training datasets.

Training Dataset	Cross-Entropy Loss	Accuracy (%)
VPFD	1.2789	81.15
$\text{VPFD}_{\text{MLP}}$	1.5523	80.00
$\text{VPFD}_{\text{MLP}+\text{noise}}$	1.2041	60.58
$\text{VPFD}_{\text{noise}}$	1.6507	60.15

#### 4.2.3. Impact of Cross-Domain Imputed Modalities on Classification Performance

The third experiments evaluate the VPFD dataset under four scenarios involving augmentation with reconstructed modalities derived from two auxiliary sources: FATIGUESet and MEFAR. We begin by training the fatigue detector  $f_\phi$  on the unmodified VPFD to establish baseline performance. Next, we run Algorithm 1 under three distinct configurations of

auxiliary source availability: (a) only FATIGUESet is available, which is used to impute the missing ECG modality, resulting in the variant referred to as VPFD w/ ECG; (b) only MEFAR is available, used to reconstruct the missing EEG channel, producing the variant termed as VPFD w/ EEG; and (c) both FATIGUESet and MEFAR are available, enabling the sequential reconstruction of ECG and EEG for the VPFD w/ ECG+EEG variant. In all cases, the original VPFD features are preserved, and only the missing channels are imputed and appended. Again, each dataset is split, with 80% used to train a classifier and the remaining 20% used for evaluation. To assess the robustness and generalizability of our approach across model architectures, we train three different classifiers in this experiment—MLP, LSTM, and CNN1D—on each dataset variant. This setup allows us to evaluate not only how each additional reconstructed modality—individually or in combination—contributes to downstream fatigue detection performance, but also the effectiveness of our framework across diverse classifier types.

Table 4 summarizes the classification accuracy of LSTM, CNN1D, and MLP models under the four scenarios. The results demonstrate that our targeted imputer effectively recovers missing modalities and that each added channel contributes to enriches feature extraction, thereby boosting fatigue detection performance. Importantly, this feature-level augmentation enables leveraging knowledge derived from high-fidelity but deployment-constrained sensors (e.g., ECG and EEG), thereby strengthening the performance of the practical sensor configuration (i.e., VPFD) without modifying its original features.

Table 4: Classification accuracy (%) under VPFD augmentation scenarios

Dataset	MLP(%)	LSTM(%)	CNN1D(%)
VPFD	81.47	83.61	60.34
VPFD w/ EEG	84.13	88.77	81.75
VPFD w/ ECG	84.14	86.99	81.55
VPFD w/ ECG+EEG	91.13	92.12	88.43

#### 4.2.4. Ablation of Batch Normalization and Jacobian Regularization

The fourth experiments, summarized in Table 5, examines how different regularization strategies influence the quality of imputed modalities, ultimately, the resulting classification performance. The MLP classifier is used

as the testbed in this experiment. An ablation study compares four settings—Batch Normalisation (BN) alone, Jacobian-norm regularization alone, both combined, and neither. BN smooths the feature distribution, while the Jacobian term sharpens the network’s sensitivity to the subtle variations required for reconstructing missing channels. When applied together, these mechanisms complement each other: BN provides a stable representation space and the Jacobian constraint enhances gradient information, allowing the model to recover absent modalities most faithfully and to achieve the best overall accuracy. This complementary effect is particularly evident in the configuration where both auxiliary sources are available, as the inclusion of multiple reconstructed modalities (i.e., EEG+ECG) accentuates the performance gap between models with and without knowledge transfer. Although this study uses the MLP classifier for clarity of presentation, the underlying analysis indicates that the same synergy between distributional and gradient-based constraints is expected to generalize to other classifiers.

Table 5: Ablation Study Results (Accuracy %)

Method	VPFD w/ EEG	VPFD w/ ECG	VPFD w/ EEG+ECG
/	81.78	81.20	83.68
BN	82.42	81.40	85.83
Jacobian	83.28	83.60	87.35
BN+Jacobian	84.14	84.13	91.13

## 5. Conclusion

Fatigue detection is crucial in high-stake environments, where reduced alertness can have serious consequences. Despite advances in sensor technology, reliability and accessibility in real-world environments remain major challenges, as many high-end sensors, such as EEG, struggle with consistency, portability, and adaptability outside controlled settings. To address this, this paper proposes a proof-of-concept framework that enables knowledge transfer across differently instrumented sensor domains, aiming to enhance fatigue detection in real-world sensor-constrained scenarios. The experimental results provide empirical support for our hypothesis and validate the effectiveness and performance of this framework.

For proof-of-concept purposes, the current framework only employs simple regression-based imputers, which might not fully capture the intrinsic

nonlinear relationships among modalities. Nonetheless, the current framework does not explicitly model interdependencies across multiple source domains; instead, it relies on a basic cascading process for multi-source enhancement. These limitations highlight important opportunities for future research, including the development of more expressive imputation techniques and principled multi-source modeling strategies to fully leverage cross-domain structure.

## References

- [1] R. Hooda, V. Joshi, M. Shah, A comprehensive review of approaches to detect fatigue using machine learning techniques, *Chronic Diseases and Translational Medicine* 8 (1) (2022) 26–35. doi:10.1016/j.cdtm.2021.07.002.
- [2] C. Zhu, L. Cui, Y. Tang, J. Wang, The evolution and future perspectives of artificial intelligence generated content (2025). arXiv:2412.01948. URL <https://arxiv.org/abs/2412.01948>
- [3] J. J. Bird, M. Pritchard, A. Fratini, A. Ekárt, D. R. Faria, Synthetic biological signals machine-generated by gpt-2 improve the classification of eeg and emg through data augmentation, *IEEE Robotics and Automation Letters* 6 (2) (2021) 3498–3504. doi:10.1109/LRA.2021.3056355.
- [4] A. G. Habashi, A. M. Azab, S. Eldawlatly, G. M. Aly, Motor imagery classification enhancement using generative adversarial networks for eeg spectrum image generation, in: *2023 IEEE 36th International Symposium on Computer-Based Medical Systems (CBMS)*, 2023, pp. 354–359. doi:10.1109/CBMS58004.2023.00243.
- [5] H. Zeng, X. Li, G. Borghini, Y. Zhao, P. Aricò, G. Di Flumeri, N. Sciaraffa, W. Zakaria, W. Kong, F. Babiloni, An eeg-based transfer learning method for cross-subject fatigue mental state prediction, *Sensors* 21 (7) (2021) 2369.
- [6] X. Zhang, M. Zeman, T. Tsiligkaridis, M. Zitnik, Graph-guided network for irregularly sampled multivariate time series, in: *International Conference on Learning Representations, ICLR*, 2022.

- [7] G. Borghini, G. Vecchiato, J. Toppi, L. Astolfi, A. Maglione, R. Isabella, C. Caltagirone, W. Kong, D. Wei, Z. Zhou, L. Polidori, S. Vitiello, F. Babiloni, Assessment of mental fatigue during car driving by using high resolution eeg activity and neurophysiologic indices, in: 2012 Annual International Conference of the IEEE Engineering in Medicine and Biology Society, 2012, pp. 6442–6445. doi:10.1109/EMBC.2012.6347469.
- [8] G. Sikander, S. Anwar, Driver fatigue detection systems: A review, *IEEE Transactions on Intelligent Transportation Systems* 20 (6) (2019) 2339–2352. doi:10.1109/TITS.2018.2868499.
- [9] J. Hu, P. Wang, Noise robustness analysis of performance for eeg-based driver fatigue detection using different entropy feature sets, *Entropy* 19 (8) (2017). doi:10.3390/e19080385.  
URL <https://www.mdpi.com/1099-4300/19/8/385>
- [10] A. Shahid, K. Wilkinson, S. Marcu, C. M. Shapiro, Stanford sleepiness scale (sss), in: A. Shahid, K. Wilkinson, S. Marcu, C. M. Shapiro (Eds.), *STOP, THAT and One Hundred Other Sleep Scales*, Springer New York, New York, NY, 2012, pp. 369–370.
- [11] E. Smets, B. Garssen, B. Bonke, J. De Haes, The multidimensional fatigue inventory (mfi) psychometric qualities of an instrument to assess fatigue, *Journal of psychosomatic research* 39 (3) (1995) 315–25.
- [12] F. B. Ortega, J. R. Ruiz, V. España-Romero, G. Vicente-Rodriguez, D. Martínez-Gómez, Y. Manios, L. Béghin, D. Molnar, K. Widhalm, L. A. Moreno, M. Sjöström, M. J. Castillo, The international fitness scale (ifis): usefulness of self-reported fitness in youth, *International Journal of Epidemiology* 40 (3) (2011) 701–711. doi:10.1093/ije/dyr039.
- [13] V. J. Gawron, Overview of self-reported measures of fatigue, *The International Journal of Aviation Psychology* 26 (3-4) (2016) 120–131.
- [14] N. Brown, S. Bichler, M. Fiedler, W. Alt, Fatigue detection in strength training using three-dimensional accelerometry and principal component analysis, *Sports biomechanics* 15 (2) (2016) 139–150.
- [15] B. T. Jap, S. Lal, P. Fischer, E. Bekiaris, Using eeg spectral components to assess algorithms for detecting fatigue, *Expert Systems with Applications* 36 (2) (2009) 2352–2359.

- [16] S. Kar, M. Bhagat, A. Routray, Eeg signal analysis for the assessment and quantification of driver's fatigue, *Transportation research part F: traffic psychology and behaviour* 13 (5) (2010) 297–306.
- [17] S. Fu, Z. Yang, Y. Ma, Z. Li, L. Xu, H. Zhou, Advancements in the intelligent detection of driver fatigue and distraction: A comprehensive review, *Applied Sciences* 14 (7) (2024). doi:10.3390/app14073016.
- [18] R. Olaganathan, T. Holt, J. Luedtke, B. Bowen, Fatigue and its management in the aviation industry, with special reference to pilots, *Journal of Aviation Technology and Engineering* 10 (2021) 45. doi:10.7771/2159-6670.1208.
- [19] H. Al-Libawy, A. Al-Ataby, W. Al-Nuaimy, M. A. Al-Taei, Hrv-based operator fatigue analysis and classification using wearable sensors, in: 2016 13th International Multi-Conference on Systems, Signals & Devices (SSD), 2016, pp. 268–273. doi:10.1109/SSD.2016.7473750.
- [20] R. Markiewicz, A. Markiewicz-Gospodarek, B. Dobrowolska, Galvanic skin response features in psychiatry and mental disorders: A narrative review, *International Journal of Environmental Research and Public Health* 19 (20) (2022) 13428. doi:10.3390/ijerph192013428.
- [21] Y. Jiao, C. Zhang, X. Chen, L. Fu, C. Jiang, C. Wen, Driver fatigue detection using measures of heart rate variability and electrodermal activity, *IEEE Transactions on Intelligent Transportation Systems* 25 (6) (2024) 5510–5524. doi:10.1109/TITS.2023.3333252.
- [22] K. Mohanavelu, R. Lamshe, S. Poonguzhali, K. Adalarasu, M. Jagannath, Assessment of human fatigue during physical performance using physiological signals: A review, *Biomedical and Pharmacology Journal* 10 (4) (2017) 1887–1896.
- [23] F. Nasirzadeh, M. Mir, S. Hussain, M. Tayarani Darbandy, A. Khosravi, S. Nahavandi, B. Aisbett, Physical fatigue detection using entropy analysis of heart rate signals, *Sustainability* 12 (7) (2020) 2714.
- [24] M. M. Bundele, R. Banerjee, Detection of fatigue of vehicular driver using skin conductance and oximetry pulse: a neural network approach, in: *Proceedings of the 11th International Conference on Information Integration and web-based applications & services*, 2009, pp. 739–744.

- [25] L. J. Trejo, K. Kubitz, R. Rosipal, R. L. Kochavi, L. D. Montgomery, Eeg-based estimation and classification of mental fatigue, *Psychology* 6 (5) (2015) 572–589.
- [26] S.-Y. Cheng, H.-T. Hsu, Mental fatigue measurement using eeg, in: *Risk management trends*, IntechOpen, 2011.
- [27] T. G. Monteiro, C. Skourup, H. Zhang, Using eeg for mental fatigue assessment: A comprehensive look into the current state of the art, *IEEE Transactions on Human-Machine Systems* 49 (6) (2019) 599–610.
- [28] J. LaRocco, M. D. Le, D.-G. Paeng, A systemic review of available low-cost eeg headsets used for drowsiness detection, *Frontiers in neuroinformatics* 14 (2020) 553352.
- [29] R. Shashidhar, S. Hariprasad, B. SHRUTHI, R. S. KAVITA, Real-time fatigue detection using a low cost wireless eeg device, *i-Manager’s Journal on Embedded Systems* 8 (2) (2020) 8–13.
- [30] F. Liu, D. Chen, J. Zhou, F. Xu, A review of driver fatigue detection and its advances on the use of rgb-d camera and deep learning, *Engineering Applications of Artificial Intelligence* 116 (2022) 105399. doi:<https://doi.org/10.1016/j.engappai.2022.105399>.
- [31] Y. Yi, Z. Zhou, W. Zhang, M. Zhou, Y. Yuan, C. Li, Fatigue detection algorithm based on eye multifeature fusion, *IEEE Sensors Journal* 23 (7) (2023) 7949–7955. doi:10.1109/JSEN.2023.3247582.
- [32] W. Deng, R. Wu, Real-time driver-drowsiness detection system using facial features, *IEEE Access* 7 (2019) 118727–118738. doi:10.1109/ACCESS.2019.2936663.
- [33] Z. Sun, Y. Miao, J. Y. Jeon, Y. Kong, G. Park, Facial feature fusion convolutional neural network for driver fatigue detection, *Engineering Applications of Artificial Intelligence* 126 (2023) 106981. doi:<https://doi.org/10.1016/j.engappai.2023.106981>.
- [34] Y. Xing, C. Lv, Z. Zhang, H. Wang, X. Na, D. Cao, E. Velenis, F.-Y. Wang, Identification and analysis of driver postures for in-vehicle driving activities and secondary tasks recognition, *IEEE*

Transactions on Computational Social Systems 5 (1) (2018) 95–108.  
doi:10.1109/TCSS.2017.2766884.

- [35] S. Yanqing, D. Pengfei, Z. Yangjing, C. Shitao, Z. Nanning, Privacy protection of sensitive bioinformation based on event cameras, Strategic Study of CAE 26 (1) (2024). doi:10.15302/J-SSCAE-2024.01.017.
- [36] K. Krejtz, A. T. Duchowski, A. Niedzielska, C. Biele, I. Krejtz, Eye tracking cognitive load using pupil diameter and microsaccades with fixed gaze, PloS one 13 (9) (2018) e0203629.
- [37] F. N. Biondi, F. Graf, J. Cort, Testing pupil size as a possible alternative metric of physical fatigue in automotive manufacturing tasks, Proceedings of the Human Factors and Ergonomics Society Annual Meeting 67 (1) (2023) 824–828. doi:10.1177/21695067231192895.
- [38] N. Y. Yair Morad, Hadas Lemberg, Y. Dagan, Pupillography as an objective indicator of fatigue, Current Eye Research 21 (1) (2000) 535–542. doi:10.1076/0271-3683(200007)2111-ZFT535.
- [39] L. Cui, Y. Wu, Y. Tang, Generalizable gaze synthesis for practical fatigue detection systems, in: 2024 International Conference on Cyber-Physical Social Intelligence (ICCSI), 2024, pp. 1–6. doi:10.1109/ICCSI62669.2024.10799435.
- [40] O. Kulkarni, R. Chandra, Bayes-catsi: A variational bayesian deep learning framework for medical time series data imputation (2024). arXiv:2410.01847.  
URL <https://arxiv.org/abs/2410.01847>
- [41] F. M. Zahid, C. Heumann, Multiple imputation with sequential penalized regression, Statistical Methods in Medical Research 28 (5) (2019) 1311–1327, epub 2018 Feb 16. doi:10.1177/0962280218755574.  
URL <https://doi.org/10.1177/0962280218755574>
- [42] Y. Deng, C. Chang, M. S. Ido, Q. Long, Multiple imputation for general missing data patterns in the presence of high-dimensional data, Scientific Reports 6 (1) (2016) 21689. doi:10.1038/srep21689.  
URL <https://doi.org/10.1038/srep21689>

- [43] Z. Che, S. Purushotham, K. Cho, D. Sontag, Y. Liu, Recurrent neural networks for multivariate time series with missing values, in: *Proceedings of the 2016 ACM SIGKDD International Conference on Knowledge Discovery and Data Mining*, ACM, 2016, pp. 749–758.
- [44] A. Verma, A. Kumar, An accurate missing data prediction method using lstm based deep learning for health care, *Procedia Computer Science* 167 (2019) 2414–2423.
- [45] W. Cao, D. Wang, J. Li, H. Zhou, S. Li, Y. He, Y. Liu, H. Zha, Brits: Bidirectional recurrent imputation for time series, *arXiv preprint arXiv:1805.10572* (2018).
- [46] Y. Eum, E.-H. Yoo, Imputation of missing time-activity data with long-term gaps: A multi-scale residual cnn-lstm network model, *Computers, Environment and Urban Systems* 95 (2022) 101823. doi:10.1016/j.compenvurbsys.2022.101823.
- [47] F. Zhu, F. Ye, Y. Fu, Q. Liu, B. Shen, Electrocardiogram generation with a bidirectional lstm-cnn generative adversarial network, *Scientific reports* 9 (1) (2019) 6734.
- [48] N. C. L. Kong, D. Lee, H. Do, D. H. Park, C. Xu, H. Mao, J. Chung, f-gan: A frequency-domain-constrained generative adversarial network for ppg to ecg synthesis (2024). *arXiv:2406.16896*. URL <https://arxiv.org/abs/2406.16896>
- [49] M. Kalanadhabhatta, C. Min, A. Montanari, F. Kawsar, Fatigueset: A multi-modal dataset for modeling mental fatigue and fatigability, in: H. Lewy, R. Barkan (Eds.), *Pervasive Computing Technologies for Healthcare*, Springer International Publishing, Cham, 2022, pp. 204–217.
- [50] S. Derdiyok, F. P. Akbulut, C. Catal, Neurophysiological and biosignal data for investigating occupational mental fatigue: Mefar dataset, *Data in Brief* 52 (2024) 109896. doi:<https://doi.org/10.1016/j.dib.2023.109896>.
- [51] M. Papakostas, A. Rajavenkatanarayanan, F. Makedon, Cogbeacon: A multi-modal dataset and data-collection platform for modeling cognitive fatigue, *Technologies* 7 (2) (2019). doi:10.3390/technologies7020046.

- [52] V. Markova, T. Ganchev, K. Kalinkov, Clas: A database for cognitive load, affect and stress recognition, in: 2019 International Conference on Biomedical Innovations and Applications (BIA), 2019, pp. 1–4. doi:10.1109/BIA48344.2019.8967457.
- [53] M. Gabbi, L. Cornia, V. Villani, L. Sabattini, Understanding fatigue through biosignals: A comprehensive dataset, 2024 19th ACM/IEEE International Conference on Human-Robot Interaction (HRI) (2024) 901–905.
- [54] S. Kovalenko, A. Mamonov, V. Kuznetsov, A. Bulygin, I. Shoshina, I. Brak, A. Kashevnik, Operatoreyevp: Operator dataset for fatigue detection based on eye movements, heart rate data, and video information, *Sensors* 23 (13) (2023). doi:10.3390/s23136197.
- [55] P. Schmidt, A. Reiss, R. Duerichen, C. Marberger, K. Van Laerhoven, Introducing wesad, a multimodal dataset for wearable stress and affect detection, in: Proceedings of the 20th ACM International Conference on Multimodal Interaction, ICMI '18, Association for Computing Machinery, New York, NY, USA, 2018, p. 400–408. doi:10.1145/3242969.3242985.
- [56] Y. Bu, S. Zou, V. V. Veeravalli, Tightening Mutual Information Based Bounds on Generalization Error (2019) 12.
- [57] Y. Mansour, M. Mohri, A. Rostamizadeh, Domain adaptation: Learning bounds and algorithms, arXiv preprint arXiv:0902.3430 (2009).
- [58] S. Ioffe, C. Szegedy, Batch normalization: Accelerating deep network training by reducing internal covariate shift (2015). arXiv:1502.03167. URL <https://arxiv.org/abs/1502.03167>
- [59] W. Li, S. Chen, Partial domain adaptation without domain alignment, *IEEE Transactions on Pattern Analysis and Machine Intelligence* 45 (7) (2023) 8787–8797. doi:10.1109/tpami.2022.3228937. URL <http://dx.doi.org/10.1109/TPAMI.2022.3228937>
- [60] M. Kalanadhabhatta, C. Min, A. Montanari, F. Kawsar, Fatigueset: A multi-modal dataset for modeling mental fatigue and fatigability, in: International Conference on Pervasive Computing Technologies for Healthcare, Springer, 2021, pp. 204–217.

## Appendix A. Theoretical Analysis

**Lemma 1.** [56] Suppose the loss function  $\mathcal{L}(f(x), y)$  is  $R$ -sub-Gaussian under  $x \sim \mathbb{P}$  for all  $y \in \mathcal{Y}$ , then, we have:

$$\mathcal{E}_{\mathbb{P}}(f) \leq \mathcal{E}_{\hat{\mathbb{P}}}(f) + \sqrt{\frac{2R^2}{n} I(x, y)} \quad (\text{A.1})$$

where  $n$  is the number of the training samples and  $I(x, y)$  is the mutual information between  $x$  and  $y$ .

**Theorem 1.** Assume that  $x, a$  are independent of each other,  $x \sim \mathbb{P}, a \sim \mathbb{Q}_a$ , while both being conditionally dependent on variable of  $y$ , Let the composite observation be defined as  $x^+ = [x, s], x^+ \sim \mathbb{P}_+$ , with the incorporating the variable  $a$ , the  $\mathcal{E}_{\mathbb{P}_+}$  have a tighten upper bound than  $\mathcal{E}_{\mathbb{P}}$ , the gap  $G$  is:

$$G = \Delta + \sqrt{\frac{2R^2}{n}} \left( \sqrt{I(x^+, y)} - \sqrt{I(x, y)} \right) < 0 \quad (\text{A.2})$$

where  $\Delta = \mathcal{E}_{\mathbb{P}_+} - \mathcal{E}_{\hat{\mathbb{P}}}$ . The proof is given in the Appendix. Following **Theorem 1**, it is evident that incorporating label-related features/sensors (i.e.,  $a$ ) can effectively reduce the generalization error bound, thereby enhancing the generalization performance.

**Proof:** For  $\mathcal{E}_{\hat{\mathbb{P}}}(f)$  and  $\mathcal{E}_{\hat{\mathbb{P}}_+}(f)$ , we have:

$$\begin{aligned} \mathcal{E}_{\hat{\mathbb{P}}}(f) &= \mathcal{L}(f(x), y) \\ \mathcal{E}_{\hat{\mathbb{P}}_+}(f) &= \mathcal{L}(f([x, a]), y) \end{aligned} \quad (\text{A.3})$$

note that the  $x, a$  are independent of each other,  $x, a$  are depend of  $y$ , thus, we can easily have:

$$\Delta = \mathcal{E}_{\mathbb{P}_+} - \mathcal{E}_{\hat{\mathbb{P}}} \leq 0 \quad (\text{A.4})$$

For  $\sqrt{\frac{2R^2}{n}} \left( \sqrt{I(x^+, y)} - \sqrt{I(x, y)} \right)$ , since  $\sqrt{\frac{2R^2}{n}} > 0$ ,  $I(x^+, y) \geq 0$  and  $I(x, y) \geq 0$ . Thus, The positivity or negativity of the expression can be determined by  $I(x^+, y) - I(x, y)$ . Then we have:

$$\begin{aligned} I(x^+, y) - I(x, y) &= H(Y) - H(Y|x^+) - (H(Y) - H(Y|x)) \\ &= H(Y|x) - H(Y|x^+) \end{aligned} \quad (\text{A.5})$$

where  $H(\cdot)$  is the entropy, since  $x^+ = [x, a]$ ,  $x_l, x_{\setminus l}$  are independent of each other,  $x, a$  are depend of  $y$ ,  $H(Y|x^+) - H(Y|x) < 0$ , then we have:

$$I(x^+, y) - I(x, y) = H(Y|x) - H(Y|x^+) < 0 \quad (\text{A.6})$$

According to Eq. A.6, we easily have:

$$\sqrt{\frac{2R^2}{n}} \left( \sqrt{I(x^+, y)} - \sqrt{I(x, y)} \right) < 0 \quad (\text{A.7})$$

Combining Eqs A.4 and A.7, we have:

$$G = \Delta + \sqrt{\frac{2R^2}{n}} \left( \sqrt{I(x^+, y)} - \sqrt{I(x, y)} \right) < 0 \quad (\text{A.8})$$

Thus, with the incorporates of the new sensors, the  $\mathcal{E}_{\mathbb{P}}$  have a tighten upper bound.

#### Q.E.D

**Theorem 2.** *Given a random variable  $\hat{a}$  generated from a distribution  $\mathbb{Q}_{\hat{a}}$ , and  $\hat{x}^+ = [x, \hat{a}] \sim \mathbb{Q}$ , then we have:*

$$\mathcal{E}_{\mathbb{P}_+}(f) \leq \mathcal{E}_{\hat{\mathbb{Q}}}(f) + \epsilon_{ideal} + d_{\mathcal{H}\Delta\mathcal{H}}(\mathbb{Q}_a, \mathbb{Q}_{\hat{a}}) + \sqrt{\frac{2R^2}{n} I(x, y)} \quad (\text{A.9})$$

where  $\mathcal{E}_{\hat{\mathbb{Q}}}(f)$  is the empirical generalization error over distribution  $\mathbb{Q}$ ,  $d_{\mathcal{H}\Delta\mathcal{H}}(\mathbb{Q}_a, \mathbb{Q}_{\hat{a}})$  is the  $\mathcal{H}\Delta\mathcal{H}$  distance between  $\mathbb{Q}_a$  and  $\mathbb{Q}_{\hat{a}}$ .

Before we proof the **Theorem 2**, we need the following Definition:

**Definition 1 (Disparity).** *Given two classifier  $f$  and  $f'$ , the disparity between two classifier  $f$  and  $f'$  over the distribution  $\mathbb{P}$  is as follows:*

$$\mathcal{E}_{\mathbb{P}}(f, f') = \mathbb{E}_{x \sim \mathbb{P}} [f(x) \neq f'(x)] \quad (\text{A.10})$$

**Definition 2 (Ideal Classifier).** *Given two Distribution  $\mathbb{P}$  and  $\mathbb{Q}$  the ideal classifier  $f^*$  have the minimum risk over two distributions as follows:*

$$f^* = \arg \min_f (\mathcal{E}_{\mathbb{P}}(f) + \mathcal{E}_{\mathbb{P}}(f)) \quad (\text{A.11})$$

**Definition 3 ( $\mathcal{H}\Delta\mathcal{H}$  distance).** *Given two Distribution  $\mathbb{P}$  and  $\mathbb{Q}$ , the  $\mathcal{H}\Delta\mathcal{H}$  distance between  $\mathbb{P}$  and  $\mathbb{Q}$  is defined as follows:*

$$d_{\mathcal{H}\Delta\mathcal{H}}(\mathbb{P}, \mathbb{Q}) = \sup_{f, f' \in \mathcal{H}} |\mathcal{E}_{\mathbb{P}}(f, f') - \mathcal{E}_{\mathbb{Q}}(f, f')| \quad (\text{A.12})$$

where  $\mathcal{H}$  is the Hypothesis space.

**Assumption:** the ideal classifier has a small risk.

$$\epsilon_{ideal} = (\mathcal{E}_{\mathbb{P}}(f^*) + \mathcal{E}_{\mathbb{P}}(f^*)) \quad (\text{A.13})$$

**Proof:**

By using the triangle inequalities, we have

$$\begin{aligned} \mathcal{E}_{\mathbb{P}_+}(f) &\leq \mathcal{E}_{\mathbb{P}_+}(f^*) + \mathcal{E}_{\mathbb{P}_+}(f, f^*) \\ &\leq \mathcal{E}_{\mathbb{P}_+}(f^*) + \mathcal{E}_{\mathbb{Q}}(f, f^*) + \mathcal{E}_{\mathbb{P}_+}(f, f^*) - \mathcal{E}_{\mathbb{Q}}(f, f^*) \\ &\leq \mathcal{E}_{\mathbb{P}_+}(f^*) + \mathcal{E}_{\mathbb{Q}}(f, f^*) + |\mathcal{E}_{\mathbb{P}_+}(f, f^*) - \mathcal{E}_{\mathbb{Q}}(f, f^*)| \\ &\leq \mathcal{E}_{\mathbb{Q}}(f) + \mathcal{E}_{\mathbb{Q}}(f^*) + \mathcal{E}_{\mathbb{P}_+}(f^*) + |\mathcal{E}_{\mathbb{P}_+}(f, f^*) - \mathcal{E}_{\mathbb{Q}}(f, f^*)| \end{aligned} \quad (\text{A.14})$$

According to definition of ideal classifier and  $\mathcal{H}\Delta\mathcal{H}$  distance we have:

$$\begin{aligned} \mathcal{E}_{\mathbb{P}_+}(f) &\leq \mathcal{E}_{\mathbb{Q}}(f) + \mathcal{E}_{\mathbb{Q}}(f^*) + \mathcal{E}_{\mathbb{P}_+}(f^*) + |\mathcal{E}_{\mathbb{P}_+}(f, f^*) - \mathcal{E}_{\mathbb{Q}}(f, f^*)| \\ &= \mathcal{E}_{\mathbb{Q}}(f) + \epsilon_{ideal} + |\mathcal{E}_{\mathbb{P}_+}(f, f^*) - \mathcal{E}_{\mathbb{Q}}(f, f^*)| \\ &\leq \mathcal{E}_{\mathbb{Q}}(f) + \epsilon_{ideal} + d_{\mathcal{H}\Delta\mathcal{H}}(\mathbb{P}_+, \mathbb{Q}) \end{aligned} \quad (\text{A.15})$$

According to Lemma 1, we have:

$$\mathcal{E}_{\mathbb{P}_+}(f) \leq \mathcal{E}_{\hat{\mathbb{P}}_+}(f) + \sqrt{\frac{2R^2}{n}} I(x, y) \quad (\text{A.16})$$

Note that  $\hat{x}^+ = [x, \hat{a}]$  and  $x^+ = [x, a]$ , we further have:

$$\begin{aligned} d_{\mathcal{H}\Delta\mathcal{H}}(\mathbb{P}_+, \mathbb{Q}) &\leq d_{\mathcal{H}\Delta\mathcal{H}}(\mathbb{P}, \mathbb{P}) + d_{\mathcal{H}\Delta\mathcal{H}}(\mathbb{Q}_a, \mathbb{Q}_{\hat{a}}) \\ &\leq d_{\mathcal{H}\Delta\mathcal{H}}(\mathbb{Q}_a, \mathbb{Q}_{\hat{a}}) \end{aligned} \quad (\text{A.17})$$

By plugging Lemma 1 and Eq.A.17 into Eq. A.15, we have:

$$\mathcal{E}_{\mathbb{P}}(f) \leq \mathcal{E}_{\hat{\mathbb{Q}}}(f) + \epsilon_{ideal} + d_{\mathcal{H}\Delta\mathcal{H}}(\mathbb{Q}_a, \mathbb{Q}_{\hat{a}}) + \sqrt{\frac{2R^2}{n}} I(x, y) \quad (\text{A.18})$$

**Q.E.D**

**Lemma 2.** [57] Let  $S$  and  $T$  be the source and target domains over  $\mathcal{X} \times \mathcal{Y}$ , respectively. Let  $\mathcal{H}$  be a hypothesis class, and let  $\ell : \mathcal{Y} \times \mathcal{Y} \rightarrow \mathbb{R}_+$  be a loss function that is symmetric, obeys the triangle inequality, and is bounded,  $\forall (y, y') \in \mathcal{Y}^2, \ell(y, y') \leq M$  for some  $M > 0$ . Then, for  $h_S^* = \arg \min_{h \in \mathcal{H}} R_S^\ell(h)$  and  $h_T^* = \arg \min_{h \in \mathcal{H}} R_T^\ell(h)$  denoting the ideal hypotheses for the source and target domains, we have

$$\forall h \in \mathcal{H}, R_T^\ell(h) \leq R_S^\ell(h, h_S^*) + d_{\mathcal{H}\Delta\mathcal{H}}(\mathbb{P}_S, \mathbb{P}_T) + \epsilon, \quad (\text{A.19})$$

where  $R_S^\ell(h, h_S^*) = \mathbb{E}_{x \sim S_X} \ell(h(x), h_S^*(x))$  and  $\epsilon = R_T^\ell(h_T^*) + R_S^\ell(h_T^*, h_S^*)$ .

**Theorem 3.** Let  $\mathcal{H}$  be a hypothesis class.  $R_s^\ell(g)$  and  $R_T^\ell(g)$  denote the expected loss of loss function  $\ell$  for the source and target domains. for  $g_s^* = \arg \min_{g \in \mathcal{H}} R_s^\ell(g)$  and  $g_T^* = \arg \min_{g \in \mathcal{H}} R_T^\ell(g)$  denoting the ideal hypotheses for the source and target domains, we have

$$R_T^\ell(g_s) \leq R_S^\ell(g_s, g_s^*) + d_{\mathcal{H}\Delta\mathcal{H}}(\mathbb{P}_T^\cap, \mathbb{P}_s^\cap) + \epsilon, \quad (\text{A.20})$$

where  $R_S^\ell(g_s, g_s^*) = \mathbb{E}_{x \sim \mathbb{P}_s} \ell(g_s(x), g_s^*(x))$  and  $\epsilon = R_T^\ell(g_T^*) + R_S^\ell(g_T^*, g_s^*)$ .

**Proof:** The proof of Theorem 3 can be obtained by substituting the variables in Lemma 2, so the proof is omitted.